

Influence of substrate surface reconstruction on the growth and magnetic properties of Fe on GaAs(001)

E. M. Kneedler, B. T. Jonker, P. M. Thibado,* R. J. Wagner, B. V. Shanabrook, and L. J. Whitman
Naval Research Laboratory, Washington, DC 20375-5343

(Received 13 March 1997)

We have studied the magnetic and structural properties of epitaxial bcc Fe(001) films grown at 175 °C on molecular-beam epitaxy-prepared GaAs(001)- 2×4 and - $c(4\times 4)$ reconstructed surfaces, with film thicknesses ranging up to ~ 30 ML (~ 43 Å). We present measurements of the thickness-dependent evolution of the magnetic properties of the Fe films as determined by *in situ* magneto-optic Kerr effect. We find that the magnetic properties and growth mode are similar for both 2×4 and $c(4\times 4)$ reconstructions, although the initial adsorption sites and island nucleation as measured by scanning tunneling microscopy are clearly dominated by the substrate surface reconstruction. The onset of room-temperature ferromagnetism occurs at 6 ML for growth on both GaAs surface reconstructions. At this coverage, the measured Curie temperature (~ 100 °C) is significantly reduced from that of bulk α -Fe (770 °C). The anisotropy is dominated by a uniaxial component such that the two $\langle 110 \rangle$ axes are inequivalent for all coverages studied. Shape anisotropy does not appear to play a significant role. [S0163-1829(97)08037-5]

INTRODUCTION

The growing interest in the behavior of magnetic thin films on semiconductor substrates is due in part to the potential for spin-sensitive heterostructure devices. The metal/semiconductor interface is expected to have a strong influence on the magnetic and electronic properties of the heterostructure.¹ Previous work has shown that high-quality epitaxial growth of (bcc) Fe can be achieved on GaAs(110) and (001), due in part to the fact that the bcc Fe lattice constant is approximately half that of zinc-blende GaAs ($2a_{\text{Fe}}/a_{\text{GaAs}} = 1.013$).^{2,3} *Ex situ* magnetic measurements of Fe films greater than 25 Å thick grown on oxide-desorbed GaAs(001) substrates have shown that such films often have an in-plane uniaxial component to the magnetic anisotropy,⁴ although an ideal bcc Fe(001) film should have fourfold symmetry. There are a number of mechanisms which may contribute to the evolving magnetic anisotropy of the Fe film, including shape anisotropy, epitaxial strain, step anisotropies, or interfacial compound formation, but the source of the uniaxial component remains an open issue. The obvious influence of the substrate raises the question of how important the initial substrate surface reconstruction is to the magnetic behavior. We report here the results for the growth of Fe films on the As-rich reconstructions of GaAs(001).

In a previous study, we reported the structure and composition of Fe films grown on GaAs(001)- 2×4 .^{5,6} This As-terminated substrate surface is commonly used as a basis for the growth of compound semiconductor device structures. The molecular-beam epitaxy (MBE)-prepared samples were characterized *in situ* with scanning tunneling microscopy (STM), photoelectron diffraction (PED), and x-ray photoelectron spectroscopy (XPS). The substrate reconstruction was shown to have a significant impact on the early growth morphology of the Fe films. From STM images, initial Fe adsorption was observed on the As-dimer rows. Monolayer islands grew laterally with increasing Fe coverage, with

more rapid growth in the $[\bar{1}10]$ direction (i.e., along the dimer rows). Island shape anisotropy was seen for Fe films as thick as 50 ML. We concluded from PED polar angle scans that the growth mode is approximately layer-by-layer (with ~ 1 ML roughness), in contrast to the pronounced three-dimensional clustering observed for growth on the (110) surface.⁷ Outdiffusion of both As and Ga into the Fe layer was evident from XPS measurements, and a persistent As signal indicated As segregation at the surface. In light of these data, the following model was proposed for the first few monolayers of growth: following island nucleation and coalescence, by 2 ML the Fe displaces the half monolayer of As surface dimers and the first monolayer of Ga atoms to form a uniform Fe/As interface.

In this paper we present a study involving a direct comparison of Fe growth on two different, well-characterized surface reconstructions of the GaAs(001) substrate: the As-dimer terminated 2×4 and $c(4\times 4)$. *In situ* magneto-optical Kerr effect (MOKE) measurements⁸ are used to follow the evolution of the magnetization in these thin-film heterostructures as a function of temperature and film thickness. Scanning tunneling microscopy (STM), photoelectron diffraction (PED), and x-ray photoelectron spectroscopy (XPS) provide a detailed picture of the initial Fe film nucleation and evolution of the interfacial structure on each surface.

EXPERIMENT

Currently accepted models for the 2×4 and $c(4\times 4)$ surface reconstructions are shown in Fig. 1.^{9,10} The terminating layer for both reconstructions is characterized by As dimerization. The 2×4 surface consists of 0.5 ML As in the form of dimers atop the first Ga layer [Fig. 1(a)] while the $c(4\times 4)$ reconstruction is more As rich, with 0.75 ML of As (as dimers) on a full ML of As, which is in turn atop the first Ga layer. The dimer bond on the 2×4 surface is parallel to the $[110]$ axis, while on the $c(4\times 4)$ surface it is parallel to the $[110]$ axis as a result of the orientation of the dangling

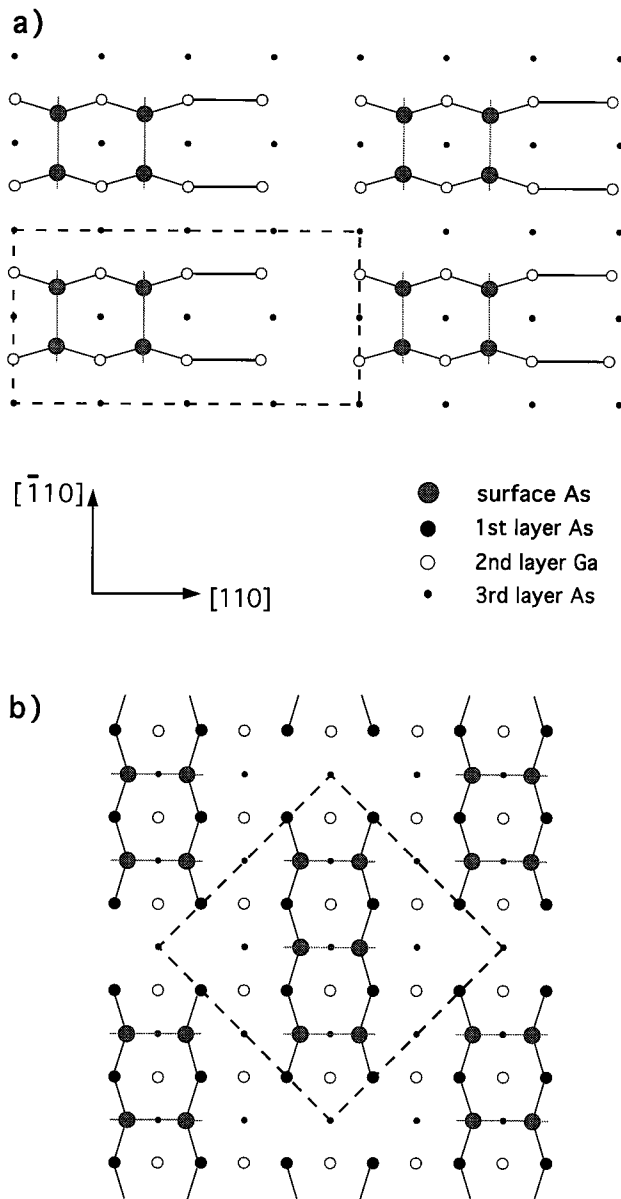


FIG. 1. Model of the As-dimer terminated (a) GaAs(001)- 2×4 and (b) $c(4\times 4)$ reconstructed surfaces, with the dashed line indicating the unit cells.

bonds for each termination. A notable distinction between the two reconstructions is the degree of spatial anisotropy in the surface structure. The 2×4 surface has a pronounced rowlike structure along $[\bar{1}10]$ due to the missing As-dimer rows, while on the $c(4\times 4)$ surface the As-dimer trios are distributed in a more spatially isotropic fashion, so that the symmetry of the $c(4\times 4)$ surface net is higher than that of the 2×4 .

The experiments were conducted in a multichamber ultra-high vacuum (UHV) molecular-beam epitaxy and surface analysis facility which included two MBE chambers, a PED/XPS/MOKE chamber, and an STM chamber, all interconnected by a UHV sample transfer system. The preparation of the GaAs(001) surface began with homoepitaxial growth of a buffer layer which exhibited a 2×4 -As surface reconstruction.⁵ This enabled the unambiguous confirmation of the $[110]$ and $[\bar{1}10]$ azimuths from the corresponding

reflection high-energy electron-diffraction (RHEED) patterns, as labeled in Fig. 1(a). The 2×4 reconstruction was achieved by cooling the sample from 580 to 550 °C under an As flux, then cooling to 200 °C under no flux prior to transfer. To produce the $c(4\times 4)$ -reconstructed surface, an As flux was maintained while cooling to ~ 400 °C. These procedures consistently produced an atomically flat, well-ordered, As-dimer terminated surface as indicated by RHEED and confirmed by STM, with average terrace widths of 0.25 to 0.5 μm for both surface reconstructions.⁶

Fe deposition was performed in a second MBE chamber using a high-temperature Knudsen cell source at a rate of 0.05 monolayer (ML)/s. We define 1 ML $\equiv 1.22 \times 10^{15}$ atoms/cm², corresponding to the atomic density of the bcc Fe(001) plane, which is approximately twice the atomic density of the bulk-terminated GaAs(001) surface (and would produce a film ~ 1.4 Å thick if deposited uniformly). The substrate temperature was 175 °C for all Fe depositions, resulting in single-crystal growth with the crystallographic axes of the Fe(001) film coincident with those of the substrate. The source was regularly calibrated by x-ray fluorescence measurements performed on thick films (~ 50 Å). Relative Fe coverages were also confirmed by XPS.

After Fe growth the sample was cooled to room temperature and transferred to either a UHV chamber outfitted with an *in situ* MOKE apparatus and an angle-resolved XPS system, or to the STM chamber. Longitudinal MOKE measurements were performed using a linearly polarized and chopped He-Ne laser beam which was reflected from the sample with an angle of incidence 22° from normal through strain-free viewports. The reflected beam passed through an analyzing polarizer, rotated 1.6° from extinction, and was detected with a photodiode. Prior to each sweep, the magnet was ramped to -500 Oe, then back to a specified field extremum $-H_{\text{max}}$. Data were then collected at specified field increments as the field was stepped at 1 s intervals from $-H_{\text{max}}$ to H_{max} to $-H_{\text{max}}$, after which the magnet was ramped back to zero field. Sweeps generally lasted 3–5 min each, and up to five sweeps were averaged for a given Kerr loop for data presented in this paper.

RESULTS AND DISCUSSION

Room-temperature longitudinal MOKE loops with the field applied along the principal symmetry axes for Fe/GaAs(001)- 2×4 are shown in Fig. 2. Along the $[110]$ axis [Fig. 2(a)], no ferromagnetic signature is detected until a coverage of 6 ML is reached, at which point a clear step in the loop signals the onset of ferromagnetic order. The coercivity is initially very low, increases to $H_c \sim 21$ Oe at 10 ML, then decreases to 14 Oe at a coverage of 16 ML. The very low coercivity observed at the onset of ferromagnetic order (6 ML) suggests that the switching of the magnetization is nearly spontaneous, indicating that thermal fluctuations are comparable to the energy required to reverse the magnetization. The loops along the $[100]$ axes [Fig. 2(b)] show similar behavior, with a clear step again appearing in the Kerr signal at ~ 6 ML. H_c increases with thickness to ~ 27 Oe then decreases to $H_c = 14$ Oe at 16 ML. The behavior in the $[\bar{1}10]$ azimuth [Fig. 1(c)] is markedly different and typical of a

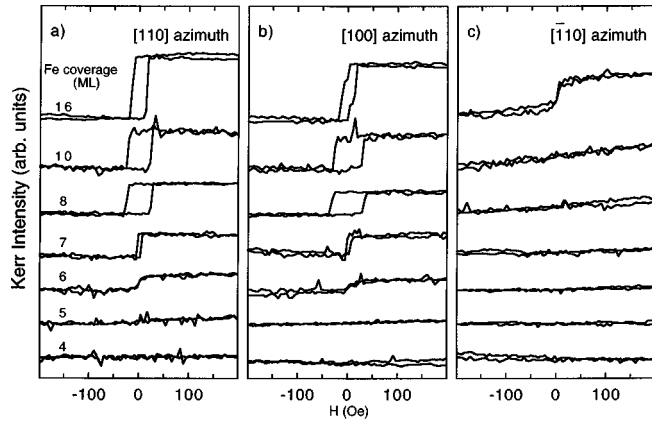


FIG. 2. Longitudinal MOKE data for Fe/GaAs(001)- 2×4 with the magnetic field applied along the (a) [110], (b) [100], and (c) $\bar{[110]}$ azimuths, taken at room temperature. Neither scaling nor smoothing were performed, and the loops are slightly offset for clarity. The vertical scale is the same for each panel.

hard axis, with no ferromagnetic hysteresis observed until a coverage of 16 ML.

It is important to note that for bulk bcc (001) Fe, the $\langle 100 \rangle$ azimuths are easy axes, and the $\langle 110 \rangle$ azimuths are *equivalent* intermediate axes, i.e., the magnetism in the (001) plane exhibits fourfold symmetry. Clearly this is not the case for the thin films studied here. A uniaxial component is observed from the onset of ferromagnetic order in which the [110] axis becomes easier and the $\bar{[110]}$ axis becomes harder. The effect is less pronounced as the thickness is increased, suggesting that the uniaxial component has its origin in the interfacial region. In the coverage range of 6 to 10 ML, the uniaxial component of the anisotropy is so dominant that the [110] axis is easier than the [100] azimuth. While it is not possible to determine the saturation magnetization from these data, the magnitude of the Kerr signal for coverages of 6 to 10 ML is consistently larger by $\sim 30\%$ for the [110] axis than for [100], and H_c is consistently smaller along [110]. Thus the uniaxial component to the anisotropy makes the [110] azimuth the easy axis of the system for coverages up to ~ 10 ML, and it remains easier than the $\bar{[110]}$ azimuth for all coverages studied.¹¹ Note that this easy axis is perpendicular to the missing dimer rows which characterize the initial surface reconstruction [Fig. 1(a)], and also to the long axis of the elongated Fe islands, as described previously.^{5,6} We therefore conclude that shape anisotropy does not play a dominant role in mediating the uniaxial component to the magnetic anisotropy in this system. By 16 ML, the easy axis switches to [100]—the squareness of the 16 ML loop indicates easy-axis behavior, and the steps observed in the loop are characteristic of an easy axis in a magnetic system with a significant uniaxial component. The larger coercivity for films of ~ 10 ML can be attributed to the greater difficulty in overcoming the hard $\bar{[110]}$ axis. Ferromagnetic resonance measurements on thicker films have confirmed that the $\langle 110 \rangle$ azimuths remain inequivalent for films up to 200 Å thick, and that the $\langle 100 \rangle$ azimuths are equivalent easy axes.⁴

The corresponding MOKE data for the Fe/GaAs(001)- $c(4\times 4)$ samples are displayed in Fig. 3, and are very similar to those obtained for the 2×4 surface. In the [110] and [100] azimuths [Figs. 3(a) and 3(b), respectively], the onset of

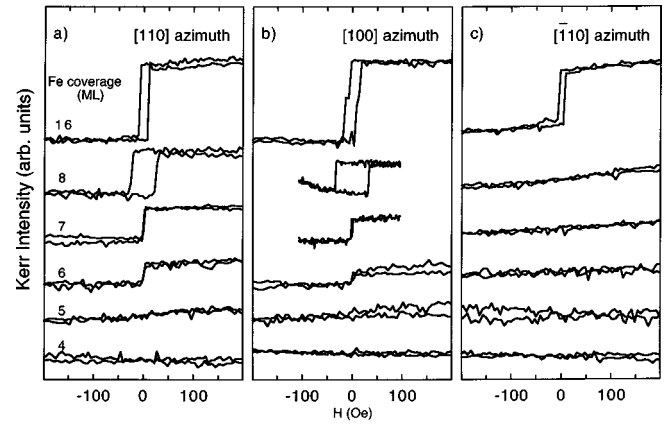


FIG. 3. Longitudinal MOKE data for Fe/GaAs(001)- $c(4\times 4)$ with the magnetic field applied along the (a) [110], (b) [100], and (c) $\bar{[110]}$ azimuths, taken at room temperature. Neither scaling nor smoothing were performed, and the loops are slightly offset for clarity. The vertical scale is the same for each panel.

room-temperature ferromagnetism again occurs at 6 ML, with near-zero coercivity. The coercivity along [110] increases to $H_c = 23$ Oe at a coverage of 8 ML, then decreases to 10 Oe by 16 ML. For the [110] axis, $H_c = 32$ Oe at 8 ML and decreases to 10 Oe at 16 ML. A comparison of Figs. 3(a) and 3(b) reveals that [110] is the easier axis for coverages less than 16 ML, based on Kerr magnitude and H_c , as was the case for the 2×4 system. The easy axis has switched to [100] at 16 ML, where steps observed in the loop are again characteristic of an easy axis in a magnetic system with a significant uniaxial component. The $\bar{[110]}$ axis shows no ferromagnetic hysteresis for coverages of 8 ML and below. At 16 ML, the [110] remanence Kerr signal is $\sim 30\%$ lower than that obtained along the other principle azimuths, and the loop rides on a positive sloping background, indicating that the saturation field is significantly higher. These data show that the $\bar{[110]}$ is again the hard in-plane axis. *Ex situ* ferromagnetic resonance measurements on the 16 ML samples confirm that the [100] azimuths are equivalent easy axes, and that the $\bar{[110]}$ axis is harder than the [110].

Temperature-dependent MOKE measurements at 6 ML reveal a reversible transition to an absence of ferromagnetic ordering above $\sim 100^\circ\text{C}$, as indicated by the disappearance of the square step in the MOKE loop. Thus the Curie temperature at 6 ML is $\sim 100^\circ\text{C}$, significantly reduced from that of bulk $\alpha\text{-Fe}$ (770°C). This suggests that the Curie temperature is a strong function of film thickness for films of a few ML, and it is reasonable to expect films thinner than 6 ML to exhibit ferromagnetic ordering below room temperature.^{12,13}

Remarkably, there is little distinction in the M - H characteristics between the 2×4 - and $c(4\times 4)$ -reconstructed substrates. The critical thickness for room-temperature ferromagnetism, the axis and magnitude of the uniaxial anisotropy, and the behavior of the coercivity with coverage do not differ appreciably between the two reconstructions. The uniaxial component to the magnetic anisotropy must, therefore, derive from the same mechanism in both cases, and we suggest that this is through the formation of an interfacial structure which is ultimately the same for each reconstruction. Gester *et al.*¹⁴ recently reported a uniaxial anisotropy for Fe/GaAs(001)- 4×2 with the hard axis in the [110]

azimuth, rather than along $\bar{[110]}$ as described above. Their sample was prepared by sputter-anneal cycles resulting in a Ga-terminated surface and a RHEED pattern which indicated a 4×2 reconstruction, although the average terrace width was not stated. The 4×2 -Ga surface is reported to be the Ga-dimer analog of the 2×4 -As surface with a topography characterized by missing Ga-dimer rows, but with the rows rotated 90° so that they are oriented along $[110]$.¹⁵ It is interesting to note that the hard axis is along the missing dimer row direction for both the Fe/ 4×2 -Ga surface of Gester *et al.* and our Fe/ 2×4 -As surface. They attributed the uniaxial anisotropy to the intrinsic step anisotropy of the initial 4×2 -Ga reconstruction, where it was assumed that the missing-dimer row corrugation of the initial substrate reconstruction was preserved at the Fe/GaAs interface, and the hard axis was thus along the rows. This model is not sufficient to describe our data, however. While the corrugation of the 2×4 -As reconstruction could, if preserved at the interface, produce anisotropy of the proper sign and direction, the $c(4\times 4)$ reconstruction does not exhibit such a missing-dimer rowlike structure along the $\langle 110 \rangle$ azimuth (see Fig. 1). Furthermore, the energetically favored Fe-As bonding would discourage a mixed interface including Fe-Ga bonds.⁵

To better understand the initial growth structure, submonolayer coverages of Fe on GaAs(001)- 2×4 and - $c(4\times 4)$ were studied with STM and PED to determine initial Fe bonding sites and surface morphology. Distinct differences in Fe adsorption and island nucleation are apparent between the two surface reconstructions from the earliest stages of deposition, as revealed by the STM images shown in Fig. 4. For the lowest coverages studied (0.05–0.1 ML), well ordered areas of the 2×4 or $c(4\times 4)$ reconstructed surface coexist with small islands of Fe. Figure 4(a) shows 0.1 ML of Fe on the 2×4 surface, where the bright and dark vertical rows correspond to the As-dimer and missing dimer rows, respectively [see Fig. 1(a)]. The Fe islands appear as bumps on the bright rows, indicating that Fe adsorbs on the As-rich portion of the 2×4 unit mesh and forms relatively small islands of 6–8 atoms—a detailed low coverage model has been described elsewhere.⁶ The rowlike structure of the initial reconstruction remains clearly visible in the 0.2 ML image shown in Fig. 4(b), and strongly effects the Fe growth, resulting in elongation of the Fe islands along $[110]$ at higher coverages.⁶

In contrast, the Fe islands appear substantially larger (and fewer) on the $c(4\times 4)$ surface for a given coverage. In Fig. 4(c) (0.05 ML), the As dimer trios [see Fig. 1(b)] appear as bright rectangular “bricks” on a dark background, while the Fe islands appear as brighter round patches approximately centered on a dimer trio, but with less well defined boundaries. The islands are about 1 ML in height (~ 1.5 Å) on both the 2×4 and $c(4\times 4)$ surfaces, but appear to be about 4 times larger on the $c(4\times 4)$ surface, suggesting a higher surface mobility. By a coverage of 0.2 ML, there is little evidence for the initial $c(4\times 4)$ reconstruction, and the Fe islands appear uniformly distributed. This is consistent with the higher isotropy of the $c(4\times 4)$ surface, but it is difficult to determine from these data to what extent the initial surface reconstruction controls the island distribution. These STM data show that the initial GaAs surface reconstruction profoundly influences the Fe adsorption and island nucleation.

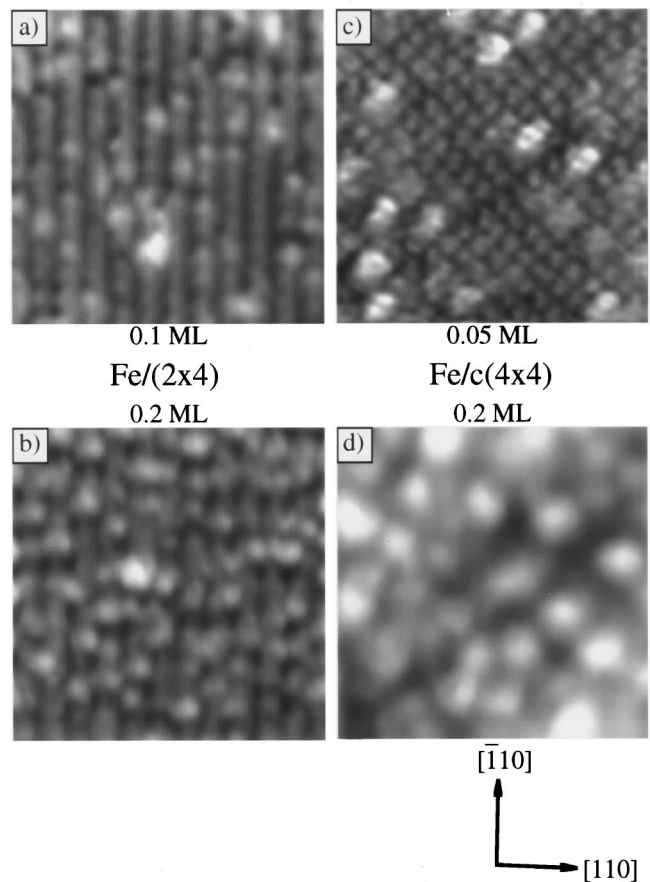


FIG. 4. STM images of (a) 0.1 ML, (b) 0.2 ML Fe/GaAs(001)- 2×4 , (c) 0.05 ML, and (d) 0.2 ML Fe/GaAs(001)- $c(4\times 4)$. Each image is 185×185 Å with $\bar{[110]}$ axis oriented in the vertical direction. The images were acquired at room temperature with a constant current of 0.1 nA and sample biases ranging from -1.8 to -3.0 V.

We see no evidence for the pyramidal surface morphology reported by Thurmer *et al.* for the epitaxial growth of Fe(001) at 400–450 K on MgO(001), which they attributed to Schwoebel barrier dominated growth.¹⁶ Our STM images show that the surface of a 35 ML (~ 50 Å) Fe film (the highest coverage studied) grown at 175°C on the GaAs(001)- 2×4 surface has a height variation of only 2 ML (~ 3 Å).⁶ A more detailed comparison between the two systems is complicated by the As out-diffusion in the latter case,^{5,6} which is likely to influence the surface diffusion, and the lack of surface chemical data to complement the STM structural data for the Fe/MgO(001) system.¹⁶

Whereas STM shows marked differences in Fe island nucleation, corresponding PED data reveal that the local atomic structure and subsequent growth more appear to be quite similar for the two reconstructions. From forward-scattering PED measurements of Fe/GaAs(001)- 2×4 with thicknesses ranging from 0.25 to 4 ML it was concluded that the growth mode is predominantly layer-by-layer, with monolayer roughness.⁵ PED data for the Fe/ $c(4\times 4)$ system show similar results, suggesting that the atomic-scale structure of the final interface may be independent of the reconstruction. However, attempts to fit these data quantitatively with single-scattering calculations¹⁷ have been unsuccessful thus far, and a more detailed study is currently under way.

XPS core-level data provide additional insight into the

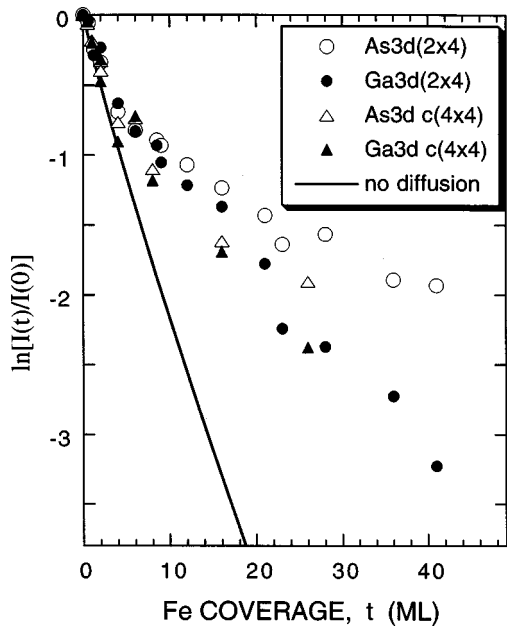


FIG. 5. Reduced intensities (defined as $\ln[I(t)/I(0)]$, where I is the integrated core-level intensity and t is the thickness of Fe deposited) of As $3d$ and Ga $3d$ core levels. The solid line is a calculation assuming two-dimensional growth without interdiffusion, an electron mean free path of 20 \AA , and the analyzer configured such that its axis is 15° out of the sample plane and its acceptance angle is 30° .

chemistry of the interface and outdiffusion of substrate species at the growth temperature of 175°C . Core-level measurements for As $3d$ and Ga $3d$ levels were obtained as a function of Fe coverage for both (2×4) and $c(4\times 4)$ reconstructions. Reduced intensities (defined as $\ln[I(t)/I(0)]$, where I is the integrated core level intensity and t is the thickness of Fe deposited) are displayed in Fig. 5. The data were obtained using monochromatized Al $K\alpha$ radiation ($\Delta E \sim 0.5 \text{ eV}$) and an electron analyzer with an acceptance angle of 30° . The analyzer axis was set at an angle of 15° relative to the sample surface to enhance surface sensitivity. The solid curve is a calculated result assuming ideal two-dimensional (2D) growth and a photoelectron mean free path $\lambda = 20 \text{ \AA}$,¹⁸ taking into account the large acceptance angle and position of the analyzer. (In the limit of an infinitesimal aperture, the curve would be linear on this plot.) For low coverages ($t \leq 2 \text{ ML}$), the substrate core-level signals are uniformly attenuated for both reconstructions, consistent with a predominantly 2D mode of Fe overlayer growth, as concluded earlier for the 2×4 surface.⁵ Thus Fe islands nucleate and coalesce to cover the substrate surface in a uniform manner on both surfaces, initially covering the As originally involved in the surface As dimers.

At higher coverages, weaker attenuation of the core-level signals indicate that growth is accompanied by outdiffusion of As, and to a lesser extent Ga. This behavior suggests that after the first 2 ML of growth, the Fe displaces substrate atom layers until it can form an interface dominated by Fe-As bonding. In the simplest model, this means until the first full plane of As atoms is reached.⁵ On the 2×4 surface, this implies dissolution of the half monolayer of As dimers and a full monolayer of Ga, while on the $c(4\times 4)$ surface

only the 0.75 ML of As surface dimers need be displaced to provide a full layer of As for bonding, leaving the subsequent monolayer of Ga intact. The interface resulting from this ideal model would be perfectly planar and characterized by Fe-As bonding with an Fe_2As stoichiometry. The coverage dependence of the core-level data for the 2×4 surface is consistent with this model. The persistence of the As signal has been attributed to surface segregated As, while the Ga signal is more rapidly attenuated with coverage, consistent with incorporation of a monolayer of Ga within the Fe film itself.⁵

Turning to the $c(4\times 4)$ surface data, we note that the Ga and As signals are generally more strongly attenuated with Fe coverage than on the 2×4 surface. This is especially striking for the As signal when one compares the initial composition of these two GaAs surface reconstructions: while the clean 2×4 surface is terminated with 0.5 ML of As (dimers) on a full layer of Ga, the $c(4\times 4)$ surface is terminated by 0.75 ML of As dimers on a full monolayer of As, which is in turn on a full layer of Ga. In the ideal Fe-As planar interface model described above, for a given Fe coverage one would expect a weaker Ga signal and a stronger As signal on the $c(4\times 4)$ than on the 2×4 . Although the Ga signal is indeed generally weaker on the $c(4\times 4)$, it is much stronger than expected from a no diffusion model (solid line), and its persistence to higher coverage indicates outdiffusion of at least a portion of the first monolayer of Ga into the Fe film. The more rapid attenuation of the As signal on the $c(4\times 4)$ is more difficult to understand, and suggests that more As is incorporated in the interface region than on the 2×4 surface. The outdiffused Ga just described may offer a means of retaining As near the interface (rather than surface segregating), in that it provides an additional stable bonding configuration for the As by reforming local patches of GaAs which are in turn covered by the Fe film with continued deposition. This scenario would produce a much more ragged and highly defected interface on the $c(4\times 4)$ surface than on the 2×4 .

SUMMARY AND CONCLUSIONS

We have compared the magnetic and structural properties of ultrathin Fe films grown at 175°C on the MBE-prepared As-dimer terminated 2×4 and $c(4\times 4)$ reconstructions of GaAs(001). The magnetic behavior was found to be very similar for the two systems. The onset of room-temperature ferromagnetic order occurs at a critical thickness of 6 ML, but with a reduced Curie temperature of 100°C , suggesting that thinner films may have Curie temperature below room temperature. A strong uniaxial component dominates the magnetic anisotropy, so that the $[110]$ azimuth becomes the unique easy axis of the system at low coverage. By 16 ML, the easy axis switches to $[100]$. The $[110]$ axis is the hard in-plane axis for all coverages studied. The STM data demonstrate that the initial GaAs surface reconstruction profoundly effects the Fe adsorption and island nucleation, and on the 2×4 surface results in the growth of islands elongated along $[110]$, i.e., along the dimer rows. However, shape anisotropy does not appear to be a dominant contribution to the magnetic anisotropy. While STM images show different island morphology, PED and XPS indicate that the growth mode and interfacial structure is quite similar for the two

reconstructions. Because the magnetic behavior is similar, we believe that the uniaxial anisotropy observed for these MBE-prepared samples derives from the same mechanism, possibly from the unidirectional nature of the Fe-As bonds at the interface or oriented Fe-As pairs within the film itself. We cannot yet rule out the possibility of a corrugated or other uniaxial interfacial structure common for growth on both the 2×4 and $c(4\times 4)$ surface reconstructions, which could in principle introduce the observed uniaxial magnetic anisotropy. Future work on the MBE-prepared 4×2 recon-

struction, which is the Ga-dimer analog of the 2×4 -As surface, will provide a valuable comparison for the results presented here.

ACKNOWLEDGMENTS

The authors gratefully acknowledge helpful discussions with J. J. Krebs. This work was supported by the Office of Naval Research.

*Present address: Physics Dept., Univ. of Arkansas, Fayetteville, AR 72701.

¹B. T. Jonker, Proc. SPIE **2140**, 118 (1994).

²G. A. Prinz and J. J. Krebs, Appl. Phys. Lett. **39**, 397 (1981).

³J. R. Waldrop and R. W. Grant, Appl. Phys. Lett. **34**, 630 (1979).

⁴J. J. Krebs, B. T. Jonker, and G. A. Prinz, J. Appl. Phys. **61**, 2596 (1987).

⁵E. Kneedler, P. M. Thibado, B. T. Jonker, B. R. Bennett, B. V. Shanabrook, and L. J. Whitman, J. Vac. Sci. Technol. B **14**, 3193 (1996).

⁶P. M. Thibado, E. Kneedler, B. T. Jonker, B. R. Bennett, B. V. Shanabrook, and L. J. Whitman, Phys. Rev. B **53**, R10 481 (1996).

⁷R. A. Dragoset, P. N. First, Joseph A. Stroschio, D. T. Pierce, and R. J. Celotta, in *Growth, Characterization and Properties of Ultrathin Magnetic Films and Multilayers*, edited by B. T. Jonker *et al.*, MRS Symposia Proceedings No. 151 (Materials Research Society, Pittsburgh, 1989), p. 193.

⁸S. D. Bader, J. Magn. Magn. Mater. **100**, 440 (1991).

⁹J. Zhou, Q. Xue, H. Chaya, T. Hashizume, and T. Sakurai, Appl. Phys. Lett. **64**, 583 (1994).

¹⁰D. K. Biegelsen, R. D. Bringans, J. E. Northrup, and L.-E. Swartz, Phys. Rev. B **41**, 5701 (1990).

¹¹In this study, MOKE data were generally taken only in the prin-

cipal crystallographic azimuths. Ferromagnetic resonance data for films >25 Å have shown that the uniaxial hard axis coincides with the $[\bar{1}10]$ azimuth to within $\pm 5^\circ$. It should be noted that the presence of a uniaxial component will generally result in a rotation of the magnetic easy direction from the $[100]$ azimuth by an amount dependent on the relative magnitudes of the uniaxial and fourfold components of the magnetic anisotropy. If the uniaxial component is sufficiently dominant (i.e., in the coverage range of 6–10 ML), the $[110]$ azimuth will be the unique easy axis.

¹²Z. Q. Qiu, J. Pearson, and S. D. Bader, Phys. Rev. Lett. **67**, 1646 (1991).

¹³G. J. Mankey, S. Z. Wu, F. O. Schumann, F. Huang, M. T. Kief, and R. F. Willis, J. Vac. Sci. Technol. A **13**, 1531 (1995).

¹⁴M. Gester, C. Daboo, R. J. Hicken, S. J. Gray, A. Ercole, and J. A. C. Bland, J. Appl. Phys. **80**, 347 (1996).

¹⁵Qikun Xue, T. Hashizume, J. M. Zhou, T. Sakata, T. Ohno, and T. Sakurai, Phys. Rev. Lett. **74**, 3177 (1995).

¹⁶K. Thurmer, R. Koch, M. Weber, and K. H. Rieder, Phys. Rev. Lett. **75**, 1767 (1995).

¹⁷D. J. Friedman and C. S. Fadley, J. Electron Spectrosc. Relat. Phenom. **51**, 689 (1990).

¹⁸M. P. Seah and W. A. Dench, Surf. Interface Anal. **1**, 2 (1979).